

Chapter 25

Mechanical Characterization and Modeling of Ceramic Foam Materials

I.M. Daniel, J.S. Fenner, and M.-Y. Chen

Abstract The materials investigated were silicon carbide foams of various densities ranging from 7.7 % to 12.3 % of the bulk material density. They were characterized under pure shear and uniaxial compression. Special test procedures were developed for this testing. For shear characterization two pairs of prismatic strips were used in a three-rail fixture. Stress–strain curves to failure were obtained from which the shear modulus, shear strength and ultimate shear strain were determined. A statistical analysis based on the Weibull distribution function was conducted to determine expected differences in results obtained by different test methods, specifically differences between three-rail shear and torsion test results. A power law model was proposed to describe the variation of shear modulus with relative density. It was also shown that the parameters of this model depend on the porosity structure of the foam for the same density. Similar tests were conducted under uniaxial compression. It was found that the Young’s modulus varies linearly with the relative density of the foam.

25.1 Introduction

Cellular materials or foams consist of different basic materials, such as metallic, polymeric or ceramic. They afford a means of optimization of mechanical and thermal properties with a minimum weight. They have been extensively discussed and reviewed in the literature. The most widely known and cited treatise on the subject is that by Gibson and Ashby [1]. An erudite review was given by Christensen [2]. Ceramic foams in particular possess a unique set of properties which make them desirable for both structural and functional applications [3–5]. Ceramic foams, such as SiC foams, are of special interest in structures exposed to severe thermal gradients. They are used as core materials in sandwich structures consisting of a ceramic matrix composite (CMC) facesheet on the high temperature side and a polymeric matrix composite (PMC) facesheet on the low temperature side. Although the foam core is primarily intended as a lightweight thermal insulator, it must have adequate stiffness and strength to maintain the integrity of the structure. Of all the factors influencing failure initiation and mode in sandwich structure, the properties of the core material are most important [6].

Open-cell ceramic foams can be produced by pyrolysis, at 1,000–1,200 °C under nitrogen, of a preceramic polymer (a silicone resin) and blown polyurethane. The morphology of the expanded polyurethane is reproduced in the final architecture of the ceramic foam. The foam takes the form of a three-dimensional array of similar size cells, where each cell tends to reach a maximum volume with a minimum surface area and surface energy (Fig. 25.1). It is widely accepted that an optimum cell geometry for low density foams is that of the Kelvin cell. This minimal surface cell proposed by Lord Kelvin is a truncated octahedron or a tetrakaidekahedron, containing 14 faces, 8 hexagons and 6 squares. During the formation of the foam, the thin membranes of each of the 14 facets fall out leaving an open cell reticulated structure consisting of interconnected struts (Figs. 25.1 and 25.2). The physical and mechanical properties of cellular materials are related to their relative density and the morphology, size, and distribution of the holes (cell windows) in the cell walls.

I.M. Daniel (✉) • J.S. Fenner
Northwestern University, Evanston, IL, USA
e-mail: imdaniel@northwestern.edu; JoelFenner2012@u.northwestern.edu

M.-Y. Chen
AFRL, WPAFB, Dayton, OH, USA
e-mail: Ming-Yung.Chen@wpafb.af.mil

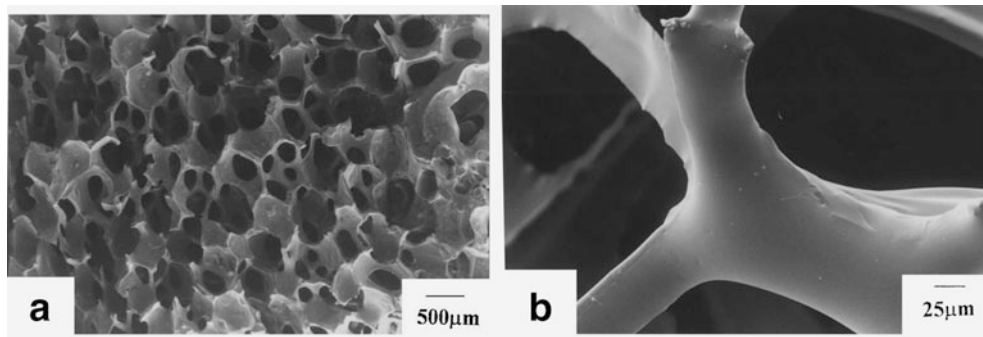


Fig. 25.1 Scanning electron micrographs of a pyrolyzed SiC foam showing (a) cell structure, (b) strut surface [4]

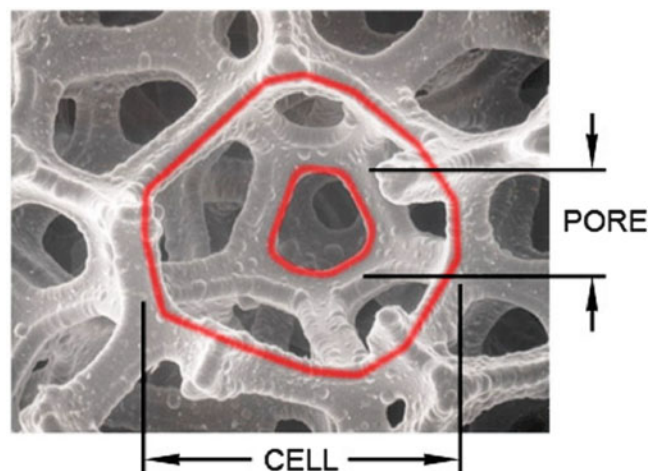


Fig. 25.2 Illustration of pore and cell geometries in a foam [7]

Since the ceramic foams under consideration are brittle materials, they are sensitive to size and stress gradients effects related to statistical distribution of strengths. Careful consideration must be given to the statistical aspects of failure when selecting, testing and designing structures with these materials. Huang and Gibson have proposed an analysis for optimizing the size and density of brittle foams [8].

This study deals with the mechanical characterization under shear and compression and modeling of four silicon carbide (SiC) foams of relative densities ranging from 4 % to 12.3 %.

25.2 Shear Characterization

The materials characterized were:

SiC foam of 7.7 % density and 65 ppi (pores per inch)

SiC foam of 12.3 % density and 65 ppi

SiC foam of 4 % density and 80 ppi

SiC foam of 10 % density and 80 ppi

Shear testing of materials in general is ideally conducted by means of torsion tests of thin wall tubes. Torsion tests of solid rods can provide information for the initial linear range of the stress–strain curve and thereby the value of the shear modulus, if a continuous record is obtained of torque versus angle of twist. However, values of ultimate shear strain and strength are

Fig. 25.3 Schematic for pure shear experiments

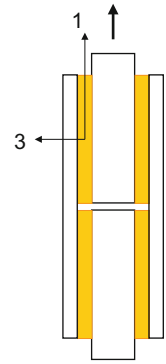
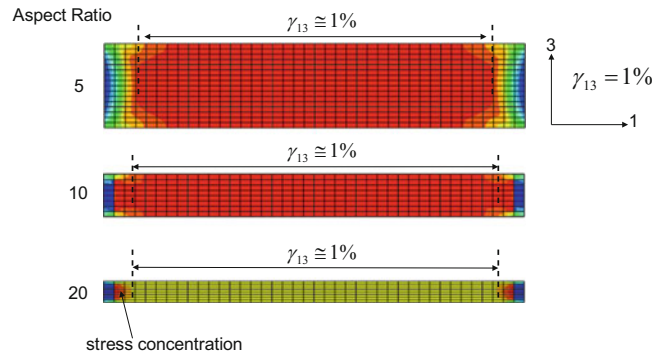


Fig. 25.4 Selection of specimen aspect ratio for shear test



affected by the nonlinear behavior and non-uniform distribution of shear stress across the cross section. An easier approach to getting shear stress–strain curves to failure is the rail shear test, provided the aspect ratio (length to thickness ratio) of specimen is high enough (Fig. 25.3) [9, 10].

An optimum aspect ratio for rail shear specimens can be determined by Finite Element Analysis as shown in Fig. 25.4 for a similar material. In general, it appears that a 10:1 aspect ratio is a reasonable choice.

For the shear test configuration shown in Fig. 25.3, the stresses are

$$\tau_{13} = \frac{P}{2A} \quad \text{and} \quad \sigma_3 = 0 \tag{25.1}$$

and the strains are

$$\gamma_{13} = \sin^{-1} \frac{d}{t} \quad \text{and} \quad \epsilon_3 = 1 - \cos \gamma_{13} \tag{25.2}$$

In the above, the shear stress and strain are along the loading direction (1-direction) and the normal stress and strain are normal to the loading direction (3-direction); P is the applied load and A is the area of the specimen attached to the rails. The specimens were strips of dimensions: 6 mm thick × 10 mm wide × 60 mm long. They were bonded to the metal rails by means of a room temperature curing epoxy adhesive (Hysol Loctite 9430). Because of the highly brittle nature of the foam materials, a special fixture was built to allow rotation along two axes at one end (Fig. 25.5). The relative displacement was measured with an extensometer mounted on the middle rails. Stress–strain curves to failure were obtained, from which the shear modulus, shear strength, and ultimate shear strain were determined. Typical stress–strain curves are shown in Fig. 25.6 for the four ceramic foams tested.

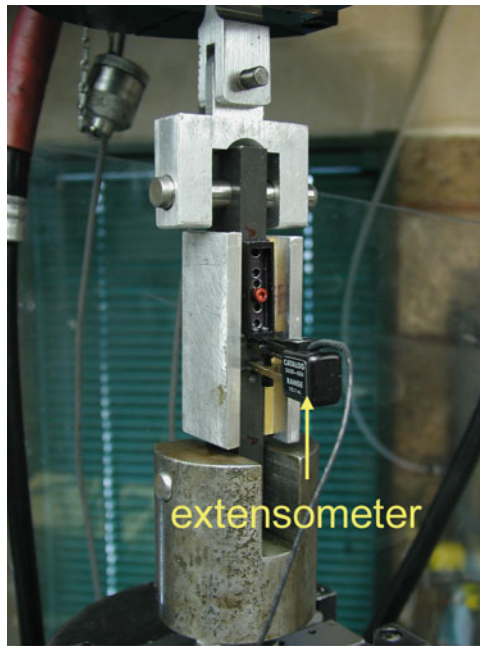


Fig. 25.5 Shear fixture with specimen in testing machine

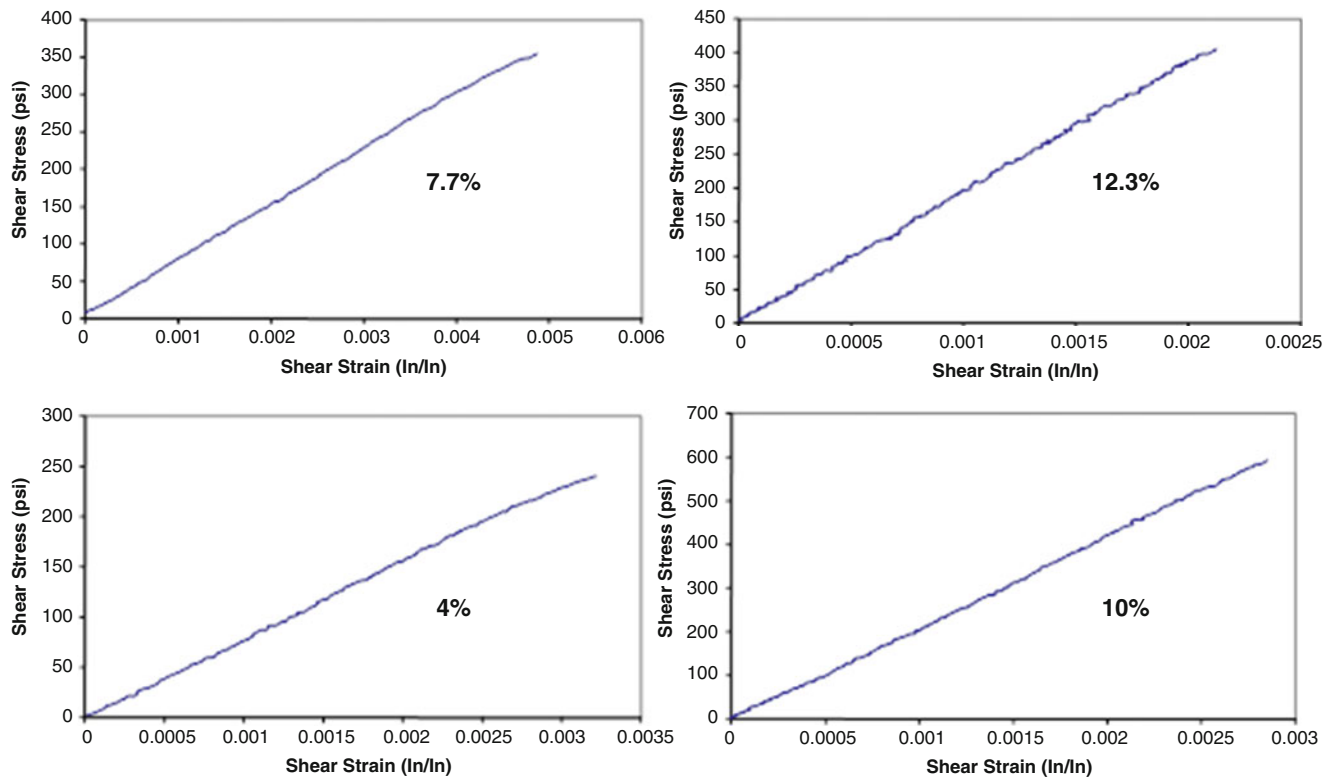


Fig. 25.6 Typical shear stress–strain curves for four ceramic foams tested

25.3 Compression Characterization

Uniaxial compression tests were conducted under stress controlled conditions using prismatic specimens with at least 2:1 aspect ratio. The aspect ratio should not be too low, because that would lead to non uniform and non uniaxial stresses, thus any modulus determination would be erroneous. A high aspect ratio might lead to buckling failure. These tests yield the complete stress–strain behavior including Young’s modulus, compressive strength and compressive ultimate strain. Of all the specimen features, the parallelism of the loading faces is the most critical. The specimen dimensions were $25 \times 12.5 \times 12.5$ mm ($1 \times 0.5 \times 0.5$ in.).

The loading fixture consists of two flat-ended cylindrical steel rods (platens) machined with ends flat and perpendicular to their axis (Fig. 25.7). The rods were 25 mm (1 in.) in diameter. Because of the high specimen stiffness and the small strains induced, it is necessary to measure accurately the displacement of the fixture platens themselves, not simply the machine crosshead. This was accomplished by using a conventional strain-gage extensometer as a displacement transducer (Fig. 25.7). Typical compressive stress–strain curves are shown in Fig. 25.8.

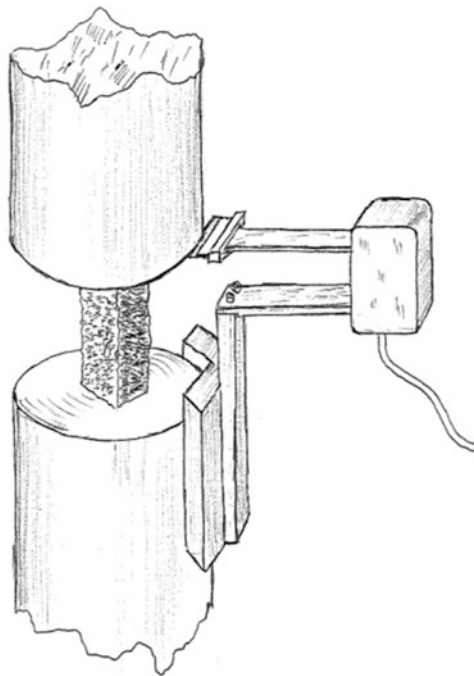


Fig. 25.7 Loading fixture with extensometer

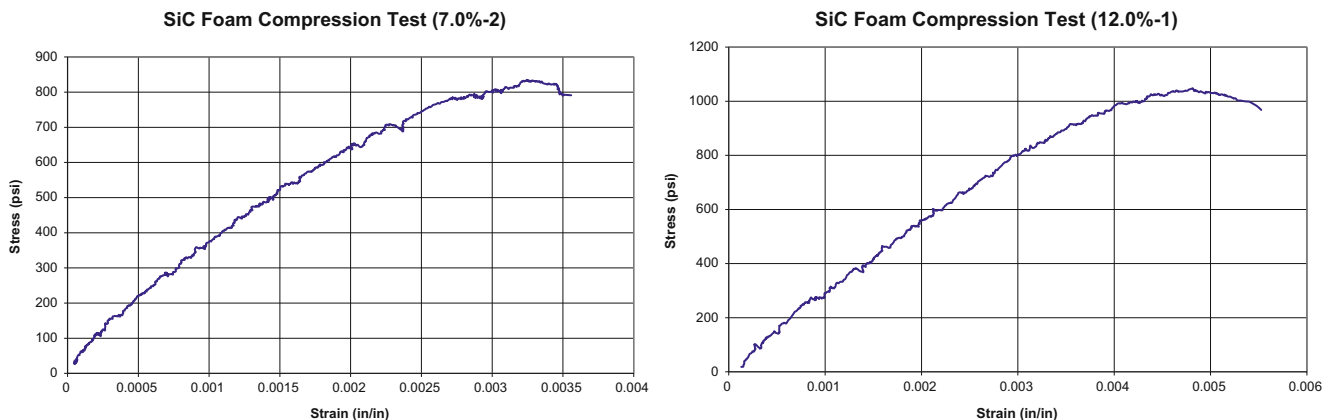


Fig. 25.8 Stress–strain curves under uniaxial compression of SiC foams of two different densities

25.4 Modeling of Elastic Behavior

The measured shear moduli and strengths were summarized in Table 25.1 below for four types of SiC foams of different densities and pores per inch (ppi), which is related to cell wall thickness. In the table below, the foam densities and moduli were normalized by the density and modulus of the bulk material. The properties of the bulk material are as follows:

Density: $\rho_b = 3,200 \text{ kg/m}^3$

Young's modulus: $E_b = 415 \text{ GPa}$ ($60 \times 10^6 \text{ psi}$)

Poisson's ratio: $\nu_b = 0.20$

Shear modulus: $G_b = 173 \text{ GPa}$ ($25 \times 10^6 \text{ psi}$)

A great deal of research has been reported on modeling of elastic and failure behavior of foams. Simple models for predicting mechanical properties are given in the classical work by Gibson and Ashby [1, 11]. The open cell of a foam is represented as a reticulated structure element (Fig. 25.9).

The relative density is defined in terms of the cell dimensions as

$$\frac{\rho}{\rho_b} = C_1 \left(\frac{t}{l} \right)^2 \quad (25.3)$$

where ρ and ρ_b are the densities of the foam and the bulk solid, respectively, t is the strut or wall thickness, l is the cell size and C_1 a constant. The ratio (t/l) is referred to as the "stockiness" ratio.

For example, a generic model for the elastic modulus in the following form has been found adequate in many cases.

$$\frac{E}{E_b} = C_2 \left(\frac{\rho}{\rho_b} \right)^n \quad (25.4)$$

Table 25.1 Shear modulus and strength of silicon carbide foams

Relative density $\left(\frac{\rho}{\rho_b} \right)$	Pores per inch (ppi)	Relative shear modulus $\left(\frac{G}{G_b} \right)$ average (range)	Average shear strength F_s (psi)
0.077	65	0.0056 $\left(\begin{array}{l} +0.0003 \\ -0.0004 \end{array} \right)$	306
0.123	65	0.0083 $\left(\begin{array}{l} +0.0007 \\ -0.0006 \end{array} \right)$	418
0.040	80	0.0037 $\left(\begin{array}{l} +0.0009 \\ -0.0006 \end{array} \right)$	192
0.100	80	0.0079 $\left(\begin{array}{l} +0.0015 \\ -0.0021 \end{array} \right)$	580

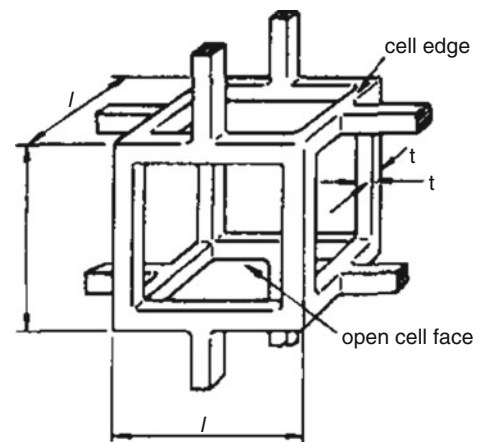


Fig. 25.9 Reticulated structure element representing a foam cell [11]

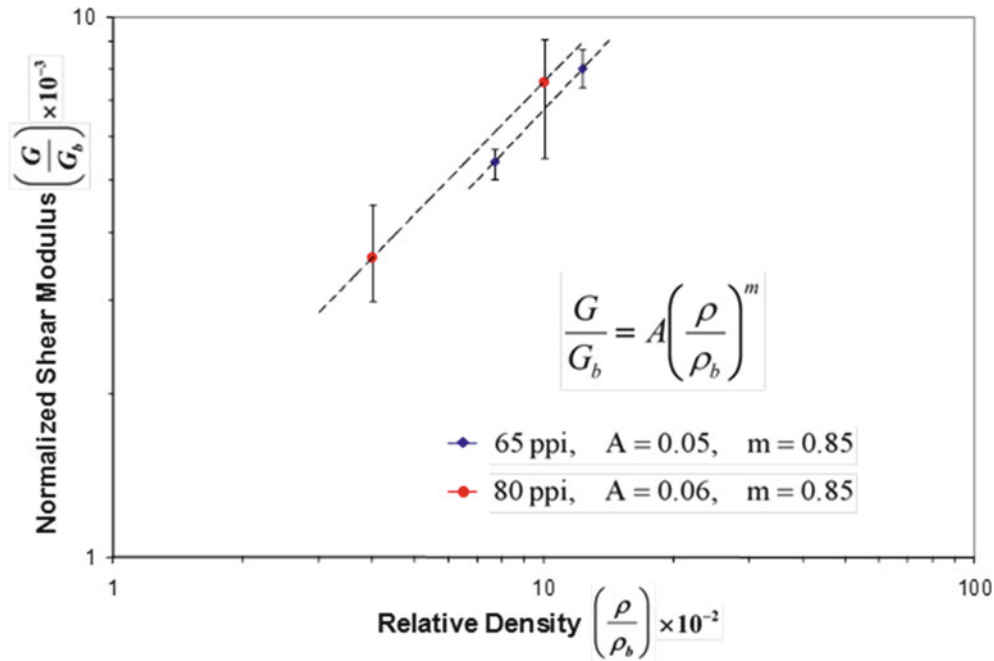


Fig. 25.10 Variation of relative shear modulus with relative density for two SiC foams

where C_2 and n are constants, E is the modulus (shear or Young's modulus of the foam), E_b the modulus of the bulk solid. Similar power law relations were proposed for the elastic collapse.

The shear modulus of the SiC foams tested could be modeled in a similar manner.

$$\frac{G}{G_b} = A \left(\frac{\rho}{\rho_b} \right)^m \quad (25.5)$$

where A and m are constants. Results of Table 25.1 were fitted to relation Eq. 25.5 as shown in Fig. 25.10. The constants obtained are:

Foam A: ppi = 65, $A = 0.05$, $m = 0.85$

Foam B: ppi = 80, $A = 0.06$, $m = 0.85$

It appears that the power exponent m depends only on the foam density regardless of the ppi property. The latter is directly related to and is roughly proportional to the cell wall thickness. It can be shown by analysis that the constant A is related to the ppi value and, thereby, to the cell wall thickness.

The average values of Young's moduli obtained from the compression tests are:

$E = 1,725$ MPa (250 ksi) and $E = 2,760$ MPa (400 ksi) for the foams of 7.7 % and 12.3 % relative densities, respectively. It is interesting to note that these moduli are proportional to the densities of the respective materials, $400/250 = 12.3/7.7$, i. e., the constants C_2 and n in Eq. 25.4 are equal to unity.

25.5 Stress Gradient Effect on Failure

A statistical analysis was conducted to determine expected differences in results obtained by different test methods, specifically differences between three-rail shear and torsion test results. Failure of brittle materials is initiated by the presence of microscopic flaws, but unlike more ductile materials, failure initiation even on a microscopic scale can be catastrophic. This is measured by the fracture toughness of the material, which is a measure of its sensitivity to defects and their size. Brittle materials such as ceramics and ceramic foams fail by the weakest link principle. Since the existence and

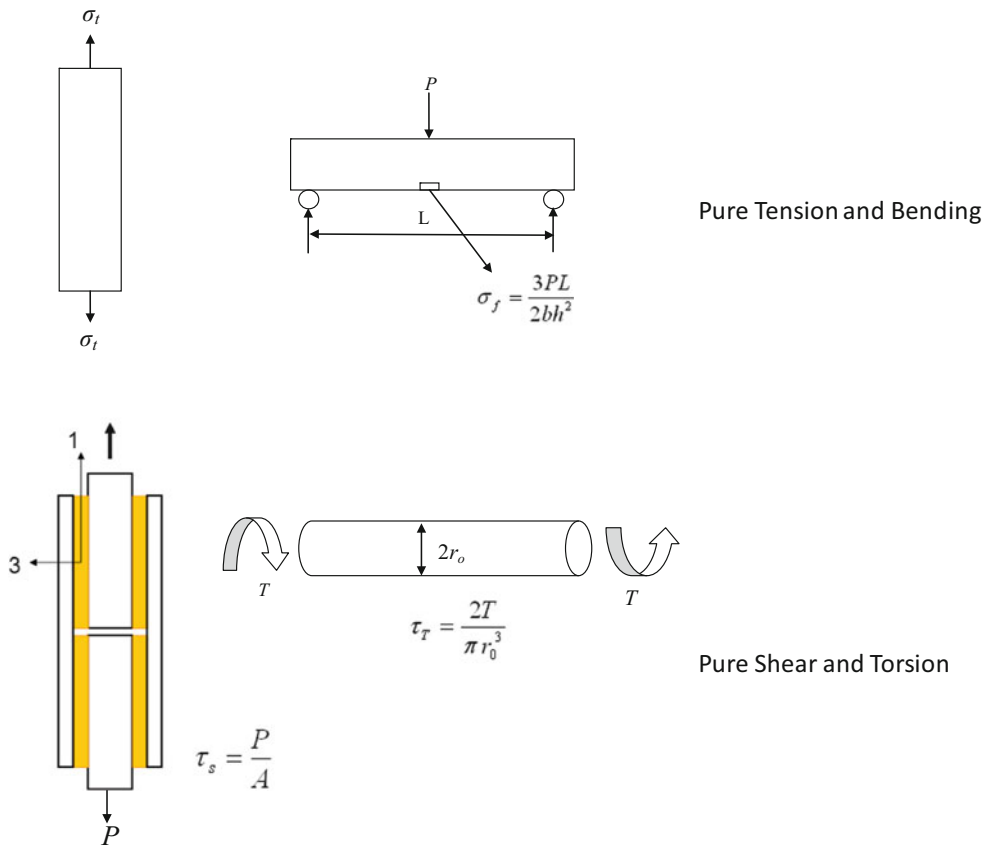


Fig. 25.11 Illustration of failure stresses under pure tension, three-point bending, pure shear, and torsion

distribution of initial defects is random, a statistical description of the scatter in the results is used. This leads to the influence of stress gradient on the failure of brittle materials [12].

The most widely used statistical distribution function is the Weibull one. According to this theory, the probability of failure at a point is given by

$$F = 1 - \exp \left\{ - \int_v \left[\frac{\sigma - \sigma_u}{\sigma_o} \right]^m dV \right\} \tag{25.6}$$

where

$F(\sigma)$ = probability of failure of material at stress σ

σ_u = zero probability strength or threshold stress below which the material never fails

σ_o = normalizing scale parameter

m = Weibull modulus or flaw density exponent that characterizes the strength of the material

V = volume of material under stress

One conservative approach is to assume that σ_u is zero. The Weibull modulus is determined by a series of tests, such as tensile, compressive or shear tests. This allows comparison of results from bending and uniaxial tensile or compressive tests and from (rod) torsion and pure shear tests (Fig. 25.11).

Assuming σ_u to be zero, for a uniformly stressed specimen (tension or compression) the probability of failure is expressed as

$$F_t = 1 - \exp \left\{ -V_t \left(\frac{\sigma_t}{\sigma_o} \right)^m \right\} \tag{25.7}$$

and, for the non-uniform stress distribution in a beam under three-point bending (assuming the material fails under tension)

$$F_f = 1 - \exp \left\{ -V_f \left(\frac{\sigma_f}{\sigma_o} \right)^m \left[\frac{1}{2(m+1)^2} \right] \right\} \quad (25.8)$$

Thus, the ratio of flexural strength to uniform tensile strength (for equal probabilities of failure) is

$$\frac{\sigma_f}{\sigma_t} = \left[2(m+1)^2 \frac{V_t}{V_f} \right]^{\frac{1}{m}} \quad (25.9)$$

If both tension and compression are equally detrimental (as in the case of ceramic foams) the probability of fracture in three-point bending is

$$F'_{ff} = 1 - \exp \left[-V_f \left(\frac{\sigma_f}{\sigma_o} \right)^m \frac{1}{(m+1)^2} \right] \quad (25.10)$$

and then, the ratio between flexural and tensile strengths is

$$\frac{\sigma'_{ff}}{\sigma_t} = \left[(m+1)^2 \frac{V_t}{V_f} \right]^{1/m} \quad (25.11)$$

For pure bending and nearly equal tensile and compressive strengths (ceramic foams) the probability of fracture is

$$F_{pf} = 1 - \exp \left[-V_f \left(\frac{\sigma_f}{\sigma_o} \right)^m \frac{1}{(m+1)} \right] \quad (25.12)$$

and the ratio of bending (pure bending) to tensile strengths is

$$\frac{\sigma_{pf}}{\sigma_t} = \left[(m+1) \frac{V_t}{V_f} \right]^{1/m} \quad (25.13)$$

The Weibull modulus (or shape parameter) m must be determined by conducting a series of tests (tension or compression) and fitting the Weibull distribution function to the cumulative failure probability data to determine the parameters. Low values of m imply high scatter and high values of m low scatter. For example, for a value of $m = 30$ (not very high scatter) and equal volumes, the strength ratios given by Eqs. 25.4, 25.6 and 25.8 are

$$\frac{\sigma_f}{\sigma_t} = 1.29, \frac{\sigma'_{ff}}{\sigma_t} = 1.26, \frac{\sigma_{pf}}{\sigma_t} = 1.12$$

For a low value of $m = 10$ (high scatter)

$$\frac{\sigma_f}{\sigma_t} = 1.73, \frac{\sigma'_{ff}}{\sigma_t} = 1.61, \frac{\sigma_{pf}}{\sigma_t} = 1.27$$

In the case of shear, the probability of failure under pure shear (rail shear test) is

$$F_s = 1 - \exp \left[-V_s \left(\frac{\tau_s}{\tau_o} \right)^m \right] \quad (25.14)$$

τ_s = shear stress

τ_o = scale parameter

M = Weibull modulus in shear

V_s = specimen volume under shear

For a solid rod under torsion the probability of failure is

$$F_T = 1 - \exp \left[-V_T \frac{2}{m+2} \left(\frac{\tau_T}{\tau_o} \right)^m \right] \quad (25.15)$$

The ratio of measured strengths by pure shear and torsion testing is

$$\frac{\tau_T}{\tau_s} = \left[\frac{m+2}{2} \frac{V_s}{V_T} \right]^{1/m} \quad (25.16)$$

The value of m must be obtained from a series of shear tests. It may be assumed equal to the value under tension or compression for quasi-isotropic ceramic foams. If, for example, $m = 30$ (low scatter) or $m = 10$ (high scatter), the strength ratios are

$$\frac{\tau_T}{\tau_s} = 1.10 \quad \frac{\tau_T}{\tau_s} = 1.20$$

25.6 Summary and Conclusions

Ceramic foams of relative densities in the range of 4–12.3 % were tested under uniaxial compression and pure shear. The materials are quasi-isotropic, behaved nearly linearly to failure and failed in a brittle manner. Moduli, strengths and ultimate strains were recorded. The Young's modulus varied linearly with relative density, whereas the shear modulus was related to relative density through a power law with an exponent slightly less than unity. An attempt to extract Poisson's ratio showed that the latter is very low or even negative.

Acknowledgement This work was supported by the Universal Technology Corporation under the US AFRL Rapid Insertion and Development of Hypersonic Materials (RIDHM) program.

References

1. Gibson LJ, Ashby MF (1997) Cellular solids: structure and properties, 2nd edn. Cambridge University Press, Cambridge
2. Christensen RM (2000) Mechanics of cellular and other low density materials. *Int J Solid Struct* 37:93–104
3. Colombo P, Modesti M (1999) Silicon oxycarbide ceramic foams from a preceramic polymer. *J Am Ceram Soc* 82(3):573–578
4. Nangrejo MR, Bao X, Edirisinghe MJ (2000) The structure of ceramic foams produced using polymeric precursors. *J Mat Sci Lett* 19:787–789
5. Bao X, Nangrejo MR, Edirisinghe MJ (2000) Preparation of silicon carbide foams using polymeric precursor solutions. *J Mater Sci* 35 (17):4365–4372
6. Daniel IM (2009) Influence of core properties on the failure of composite sandwich beams. *J Mech Mater Struct* 4(7–8):1271–1286
7. ERG (2011) Duocel-reticulated carbon, ceramic and metal foam basics. <http://www.ergaerospace.com/Description.htm>
8. Huang JS, Gibson LJ (1993) Optimum cell size and density of brittle foams. *J Mater Sci Lett* 12:602–604
9. Daniel IM, Ishai O (2006) Engineering mechanics of composite materials, 2nd edn. Oxford University Press, New York
10. Daniel IM, Cho J-M (2011) Characterization of anisotropic polymeric foam under static and dynamic loading. *Exp Mech* 51(8):1395–1403
11. Gibson LJ (1989) Modelling the mechanical behavior of cellular materials. *Mater Sci Eng A* 110:1–36
12. Daniel IM, Weil NA (1963) The influence of stress gradient upon fracture of brittle materials. ASME paper no. 63-WA-228